Neurotoxicology 74 (2019) 74–80

Contents lists available at ScienceDirect

Neurotoxicology

journal homepage: www.elsevier.com/locate/neuro

Full Length Article

Protective mechanism of Taxifolin for chlorpyrifos neurotoxicity in BV2 cells

Chen Zhang, Jichun Zhan, Mingyi Zhao, Hongmei Dai, Yuanying Deng, Wenjuan Zhou, Lingling Zhao*

Department of Paediatrics, Third Xiangya Hospital, Central South University, Changsha, Hunan, China

ARTICLE INFO

Keywords:
Taxifolin
Chlorpyrifos
BV2 cells
Oxidative stress
Inflammation
Autophagy

ABSTRACT

Chlorpyrifos (CPF) is an organophosphorus pesticide that can damage the central nervous system in children upon exposure. Taxifolin (Tax) exerts protective effects against neurotoxins; however, the mechanism has not yet been illustrated. The current study used BV2 cells to investigate the protective mechanism underlying the organophosphorus pesticide taxifolin on CPF-induced neurotoxicity, which might present a therapeutic potential for the prevention and treatment of the nervous system diseases in children. BV2 cells were randomly divided into 4 groups: DMSO, CPF, Tax, and Tax + CPF. The viability, morphocytology, oxidative stress, inflammatory reaction, and autophagocytosis have been studied in the cells using Western blot analysis, CCK-8 assay, enzyme-linked immunosorbent assay, and immunofluorescence to estimate the level of LC3 II. As a result, CPF was found to exert a significant toxic effect on BV2 cells that was characterized by rounded cell body, atrophic synapse, poor adhesion, cell aggregation, inflammation, oxidative reaction, and autophagy. Tax treatment has a protective effect on CPF-induced neurotoxicity via downregulation of ROS, TNF-α, IFN-γ, and p62 levels and increased LC3 II level, which in turn, improved the viability and activity of BV2 cells. This phenomenon suggested that Tax can reduce the inflammation and oxidative stress and promote autophagy. Furthermore, the current study suggested that the protective mechanism of Tax on CPF-induced BV2 cell toxicity was via up-regulation of pAMPK level and activation of Nrf2/HO-1 signaling pathway.

1. Introduction

Pediatric nervous system diseases are severe life-long risks to the health of children. A number of studies have shown that environmental factors are one of the causes of children's neurological diseases (Jurewicz et al., 2013). Organophosphorus pesticides are crucial environmental chemical factors; however, the mechanisms of pathogenesis are not yet clear. Therefore, investigation of the mechanisms underlying the pathogenesis of organophosphorus pesticides is vital for the prevention and treatment of chlorpyrifos (CPF)-induced neurological diseases.

CPF (leroy or parathion) is one of the most abundant and widely used pesticides worldwide (Sasikala et al., 2012). Children are rather vulnerable to the pesticide-caused severe injury because of their high susceptibility, weak ability to remove toxins, and rapid development of the disease. CPF is one of the major adverse environmental factors endangering children's health. It can not only inhibit the activity of acetylcholine esterase but also induce the occurrence of immune inflammatory response to damage the nervous system function through the blood-brain barrier (Gupta et al., 2010; Parran et al., 2005; Roncati et al., 2016).

Taxifolin (Tax) (3,5,7,3′,4′-pentahydroxy-flavanone or 2,3-dihydroquercetin) is a flavonoid, present abundantly in citrus fruits, grapes, olive oil, and onions(Marks et al., 2010; Rauh et al., 2006, 2015). As a common bioactive constituent of foods and herbs, Tax has been shown to exert a wide range of biochemical and pharmacological effects, including anti-tumor, anti-inflammatory, anti-diabetic, hepatoprotective, cardioprotective, and neuroprotective effects; also, it contributes to the prevention of Alzheimer's disease (Binukumar et al., 2011; Dutta et al., 2012; Gupta et al., 2010; Levesque et al., 2010; Liu et al., 2015a, b; Ma et al., 2012; Ozkul et al., 2007; Zhang et al., 2011). Importantly, Tax exerts significant antioxidant effects that are critical for preventing the onset of apoptosis (Kaushik et al., 2011). Moreover, it can also inhibit the oxidative enzymes and the overproduction of ROS, thereby ameliorating the cerebral ischemia-reperfusion injury (Kaur et al., 2019; Mijaljica et al., 2011).

Herein, we hypothesized that Tax might alleviate the CPF-induced oxidative stress, inflammatory response, and autophagy in BV2 cells by promoting the occurrence of autophagy, activating the Nrf2/HO-1 signaling pathway, and lowering the pAMPK level. Thus, the present

* Corresponding author at: Third Xiangya Hospital of Central South University, Department of Paediatrics, 138, Tong Zipo, Changsha, Hunan, 410013, China.
E-mail address: llzhao2011@qq.com (L. Zhao).

https://doi.org/10.1016/j.neuro.2019.05.010
Received 19 February 2019; Received in revised form 27 April 2019; Accepted 27 May 2019
Available online 29 May 2019
0161-813X/

study aimed to explore the protective mechanism of the Tax antagonistic, CPF, which induced BV2 cell neurotoxicity and to provide a theoretical basis for the prevention and treatment of neurological diseases in children.

2. Materials and methods

2.1. Cell culture and chemicals

The BV2 cell line was obtained from the Shanghai Xin Yu Biotech Co., Ltd and maintained in RPMI 1640 medium containing 10% fetal bovine serum (FBS; Sijiqing F8240-100) at 37 °C in a humidified incubator with 5% CO_2. Chlorpyrifos was purchased from Dow AgroSciences. Taxifolin was obtained from Fluka.

2.2. Cell treatment

BV2 cells were randomly divided into four groups. Group DMSO: The cells treated with 0.1% DMSO in RPMI 1640 complete medium served as the control group. The experiment was set up at different time points. CPF and Tax are fat-soluble and easily soluble in DMSO. Group CPF: Cells treated with 200 μmol/L CPF in RPMI 1640 complete medium for 6 h. Group Tax: Cells were treated with Tax-RPMI 1640 complete medium at different concentrations and time points. Group Tax + CPF: Cells were pre-treated with 100 mmol/L Tax-containing RPMI 1640 complete medium for 6 h, followed by 200 μmol/L CPF in RPMI 1640 complete medium for an additional 6 h.

2.3. Cell viability assays

The viability of the cells was determined using CCK-8 (Dojindo) assay. Briefly, the cells were plated at a density of 5×10^4 cells/mL (150 μL/well) into 96-well plates. After a specific period of incubation, a volume of 100 μL RPMI 1640 medium and 10 μL CCK-8 reagent (5 mg/mL) were added to each well. Subsequently, the plate was incubated for 2 h at 37 °C, and the absorbance was measured at 450 nm using a microplate reader (En Vision, PerkinElmer Lifesciences). Each measurement was repeated three times.

2.4. Cell morphology assay

Cells were plated into 6-well plates. The cell morphology was observed by optical microscopy.

2.5. Measurement of cellular ROS

Cells were plated into 6-well plates after CPF, Tax and Tax + CPF treated 6 h. Subsequently, the treated cells were incubated with 400 μmol/L ROS fluorescent (Beyotime C1048) dyes for 40 min at 37 °C and observed by optical microscopy to determine the level of ROS in each group.

2.6. Measurement of TNF-α and TNF-β

The concentrations of TNF-α and TNF-β released in the culture were assessed using enzyme-linked immunosorbent assay (ELISA) kits (R&D Systems) with a volume of 50 μL assay diluent; standard, control, or sample was added to each well, respectively and incubated for 2 h at room temperature. Subsequently, 100 μL conjugate and 100 μL substrate solution were added. Finally, 100 μL stop solution was added to the wells, and the absorbance was measured at 450 nm on a microplate reader with the correction wavelength set at 540 or 570 nm.

2.7. Immunofluorescence for measurement of LC3 II

The cells were fixed using fresh 4% paraformaldehyde for 30 min and permeabilized with 0.5% Triton X-100 for 30 min. After washing with PBS, the cells were incubated in bovine serum albumin (BSA; Sino-American Biotechnology Co., Ltd) for 1 h at room temperature, followed by incubation with anti-LC3 II (Proteintech) at 4 °C and a secondary antibody for 90 min at 37 °C. The cell nuclei were counterstained with DAPI for 10 min and observed under a fluorescence microscope (Leica).

2.8. Western blotting assay

The cells were suspended in lysis buffer on ice for 30 min. An equivalent of 20–100 μg protein lysate was resolved by 4% SDS-PAGE (AMRESCO) and transferred to PVDF membrane (Millipore). Then, the membrane was probed with the appropriate primary antibody at 4 °C overnight and a horseradish peroxidase (HRP)-conjugated secondary antibody for 45–60 min. The immunoblots were visualized with a chemiluminescence ECL reagent (Thermo). The primary antibodies, anti-P-AMPK (#2535 P, 1:1000) and anti-AMPK (#2603 P, 1:1000), were purchased from CST, while anti－HO-1 (10901-1-AP, 1:200), anti-Nrf2 (16396-1-AP, 1:200), anti-p62 (18420-1-AP, 1:1000), anti-LC3 (18725-1-AP, 1:500), and β-actin (20536-1-AP, 1:1000) were procured from Proteintech.

2.9. Statistical analysis

All statistical analyses were performed using the GraphPad Prism 5.0 software. Data from at least three independent experiments, each performed in triplicate, are presented as the mean ± standard deviation (SD). The significance of the differences between the groups was analyzed using one-way ANOVA. *t*-test was used to compare the average between two groups. $P < 0.05$ was considered as statistically significant.

3. Results

3.1. Effect of Tax on cell viability and morphocytology of BV2

Compared to the DMSO group, the viability of BV2 cells decreased with increasing concentration of Tax at 25, 50, 100, and 200 μmol/L after 6-h treatment ($P > 0.05$). However, the cell viability was significantly reduced at the concentration of 400 μmol/L of Tax ($P < 0.0001$) (Fig. 1A). Furthermore, the viability of BV2 cells did not exhibit a significant difference ($P > 0.05$) (Fig. 1C) after Tax treatment (100 μmol/L) for 3, 6, 12, and 24 h as compared to that in the DMSO group. However, no significant difference ($P < 0.05$) (Fig. 1D) was detected in the cell viability at the time points of 12 and 24 h as compared to the blank group. Interestingly, the cell viability in the Tax + CPF group was significantly higher than that in the CPF group ($P < 0.05$) (Fig. 1B).

Light microscopy revealed that CPF-induced BV2 cell body was round, the synapse was atrophied, adherence was weakened, and the cells vacuolated, aggregated and floated. Cells in the Tax group were similar to the DMSO group. In the Tax + CPF group, cells wall-sticking was better with their more and stronger synapse than BV2 cells in the CPF group. However, less cell vacuolation was still exist under Tax's treatment. (Fig. 2).

3.2. Effect of Tax on the oxidative stress of BV2

Fluorescence staining was used to detect the level of ROS in the cells. The DMSO group exhibited weak intensity green fluorescence, while the CPF group exhibited intense staining. Interestingly, the Tax and Tax + CPF groups presented abundant but weak intensity staining (Fig. 3A). Compared to the DMSO group, the level of ROS in the CPF group was significantly increased ($P < 0.001$), but not in the Tax and Tax + CPF groups ($P > 0.05$). On the other hand, the level of ROS

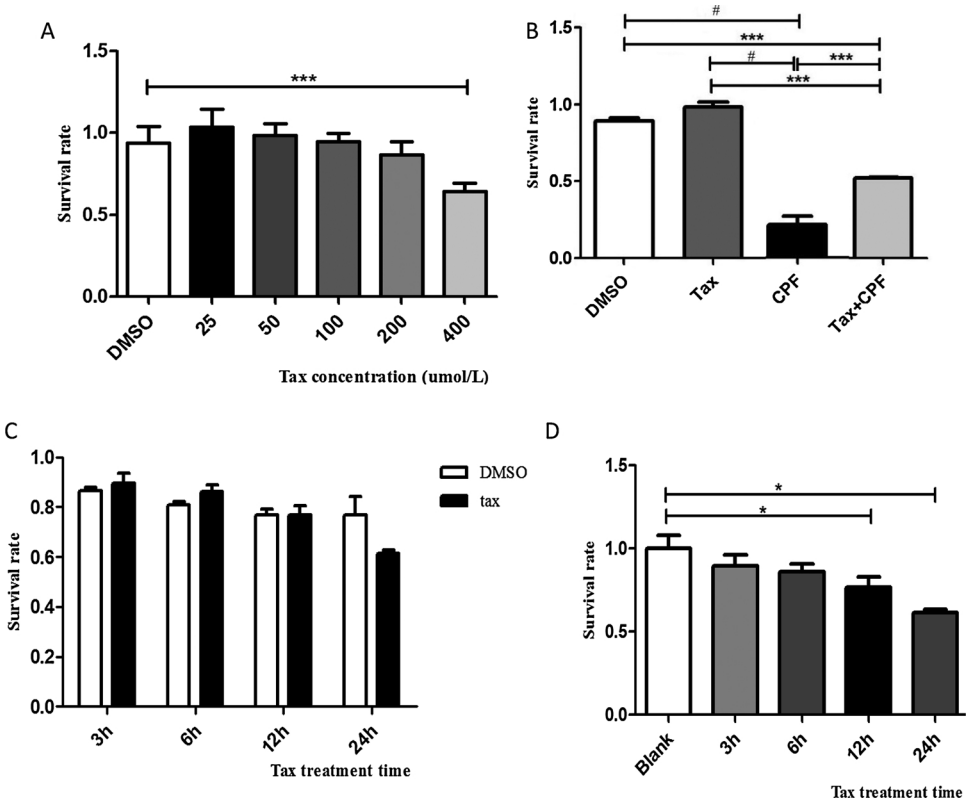

Fig. 1. CCK-8 to detect the viability and activity of BV2 cells. A: The effect of different Tax concentrations on the viability of BV2 cells. Cell viability of BV2 is significantly reduced at the concentration of 400 μmol/L Tax. **B**: the activity of BV2 cells in each group. Compared with DMSO group, cell viability of BV2 significantly reduced in CPF group, Tax + CPF group. **C&D**: The effects of Tax at different time points on the viability of BV2 cells. Compared with DMSO group, with 100 μmol/L Tax treating for 3 h, 6 h, 12 h, 24 h, cell viability of BV2 is no significant difference. Compared with Blank group, cell viability of BV2 is deceases by time, and at the time point of 12 h and 24 h, there is significant difference. $^{*}P < 0.05$, $^{***}P < 0.0001$, $\#P < 0.0001$.

significantly decreased in the Tax and Tax + CPF groups as compared to the CPF group ($P < 0.05$) (Fig. 3B).

3.3. Effect of Tax on the inflammatory reaction of BV2

In order to clarify the effect of Tax on the CPF-induced inflammatory reaction of BV2 cells, the levels of TNF-α and IFN-γ in the supernatant were detected by ELISA. The results showed that the levels of TNF-α and IFN-γ in the CPF and Tax + CPF groups were significantly increased as compared to the DMSO and Tax groups ($P < 0.05$). Compared to the CPF group, the levels of TNF-α and IFN-γ in the Tax + CPF group was markedly declined ($P < 0.05$) (Fig. 4).

3.4. Effect of Tax on the autophagocytosis of BV2

Immunofluorescence staining was used to detect the level of LC3 II

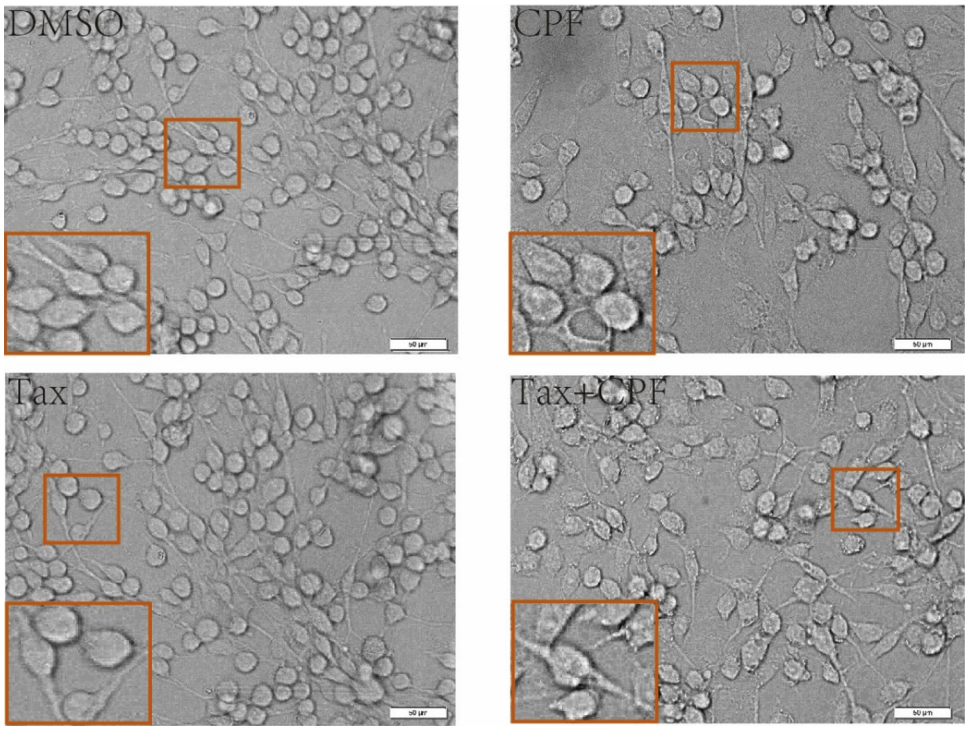

Fig. 2. The effects of Tax on morphology of BV2 were observed under light microscope (20×). Observation of BV2 cells by light microscope showed that CPF-induced BV2 cell body turned round, synapse atrophied, wall-sticking weaken, vacuolated, cell gathered and floated. Cells in the Tax group were similar to the DMSO group. In the Tax + CPF group, cells wall-sticking was better with their more and stronger synapse than BV2 cells in the CPF group. However, less cell vacuolation was still exist under Tax's treatment.

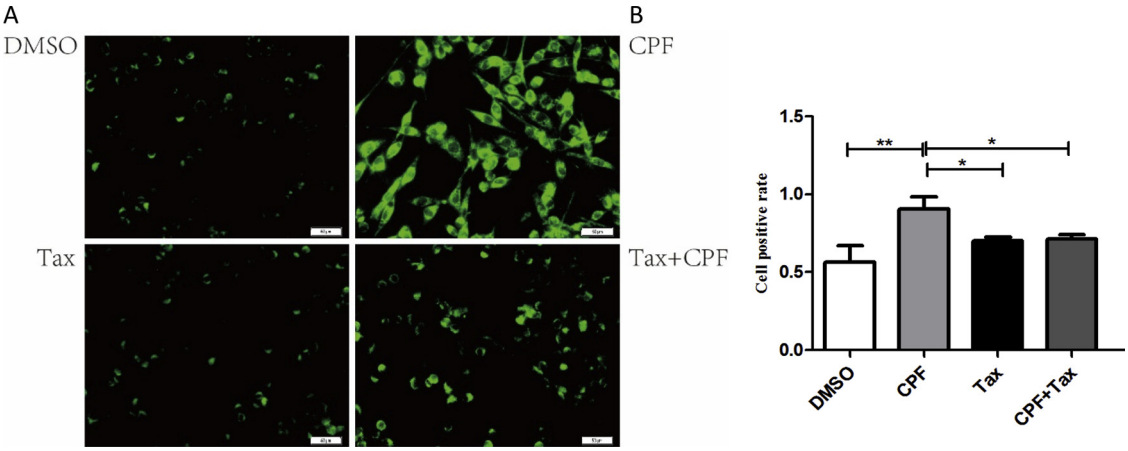

Fig. 3. Fluorescence staining to observe effect of Tax on oxidative stress of CPF-induced BV2. Fluorescence staining was used to detect ROS levels in cells and observed under fluorescence microscope. **A**: DMSO group's green fluorescence were rarely and brightness were weak, CPF group's green fluorescence were more and brightness were stronger, while Tax and Tax + CPF group's green fluorescence were more less and brightness were more weaker. **B**: Compared with DMSO group, ROS in CPF group were significantly increased, and no significant increase in Tax and Tax + CPF group. Compared with CPF group, ROS significantly decreased in Tax and Tax + CPF group, and the difference was statistically significant. *$P < 0.05$, **$P < 0.001$.

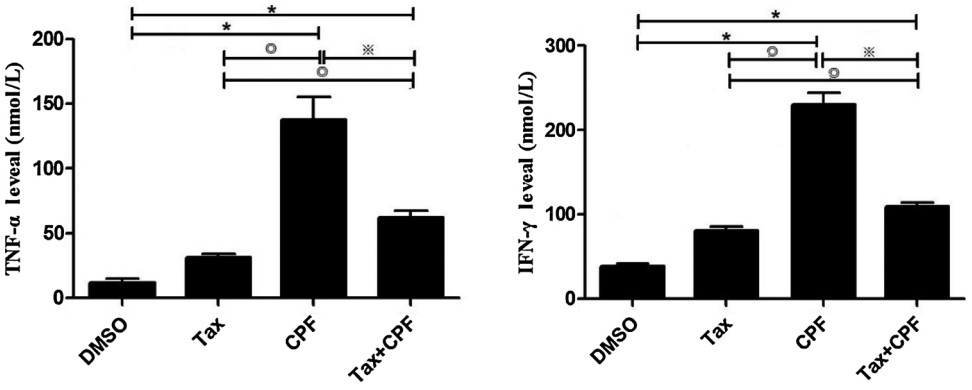

Fig. 4. Effect of Tax on the expression of TNF-α and IF**N**-γ in CPF-induced BV2 cells. The levels of TNF-α and IFN-γ in the supernatant of the cells were detected by ELISA to clarify the effect of Tax on the inflammatory reaction of BV2 cells induced by CPF. There was no statistically difference between DMSO and Tax group. The levels of TNF-α and IFN-γ in CPF and Tax + CPF group were significantly increased comparing with DMSO group, and the difference was statistically significant. Compared with CPF group, the levels of TNF-α and IFN-γ in Tax + CPF group was dramatic decline with statistically significant. *comparison with DMSO group $P < 0.05$, ※comparison with CPF group $P < 0.05$, ◎comparison with Tax group $P < 0.05$.

in BV2 cells. The green indicated positive, suggesting that LC3 II was primarily expressed in the cytoplasm. The expression of p62 and LC3 II proteins was determined by Western blotting. Compared to the DMSO group, the expression of LC3 II in the CPF group was not significantly increased in the cytoplasm, and the expression of LC3 II in both the Tax and Tax + CPF groups was increased in the cytoplasm (Fig. 5A). The level of p62 decreased in the Tax + CPF group ($P < 0.05$), while that of LC3 II was increased ($P < 0.05$) (Fig. 5B, C).

3.5. Effect of Tax on the AMPK level and Nrf2/HO-1 pathway

In the present study, Western blot was used to determine the expression of pAMPK, AMPK, Nrf2, and HO-1 proteins in BV2 cells in each group after CPF induction, as well as after blocking the AMPK pathway by compound C. The results showed that the expression of AMPK, pAMPK, Nrf2, and HO-1 in the CPF group did not alter significantly as compared to the DMSO group ($P > 0.05$). The expression of AMPK and pAMPK proteins increased in the Tax group ($P < 0.05$), while that of Nrf2 and HO-1 proteins was reduced ($P < 0.05$). In the Tax + CPF group, the expression of AMPK and pAMPK proteins was reduced ($P < 0.05$), while that of the Nrf2 protein was high ($P < 0.05$); the HO-1 protein did not show a significant increase in expression ($P > 0.05$). Compared to the CPF group, the expression of AMPK and pAMPK proteins did not increase significantly increase in the Tax group ($P > 0.05$), while that of Nrf2 and HO-1 proteins was reduced ($P < 0.05$). In the Tax + CPF group, a significant reduction was detected in the pAMPK protein expression ($P < 0.05$), an increase in the Nrf2 level ($P < 0.05$), and unaltered HO-1 expression ($P > 0.05$) (Fig. 6A, B). After the intervention of compound C for 1 h, the expression of AMPK, pAMPK, Nrf2, and HO-1 proteins were reduced in both the CPF and Tax + CPF groups as compared to the DMSO group ($P < 0.05$). In the Tax group, the expression of pAMPK, Nrf2, and HO-1 proteins was reduced significantly ($P < 0.05$), while that of AMPK did not change ($P > 0.05$). Compared to the CPF group, the expression of AMPK and pAMPK proteins was relatively higher ($P < 0.05$) and that of Nrf2 and HO-1 was lower ($P < 0.05$) in the Tax group. In the Tax + CPF group, the expression of AMPK was slightly elevated, albeit not significantly ($P > 0.05$), while that of pAMPK, Nrf2, and HO-1 decreased markedly ($P < 0.05$) (Fig. 6C, D).

4. Discussion

Chlorpyrifos is an organophosphorus insecticide with broad spectrum, high efficiency, low toxicity, low residue, and resistance. It is one of the most widely used pesticide product in domestic and international market. Individuals are exposed to CPF via respiratory as well as digestive tracts and skin mucosa. Because it is fat soluble, CPF can pass through the blood-brain barrier into the brain and also through the placental barrier into the fetal body (Parran et al., 2005; Roncati et al., 2016). As a major adverse environmental factor that endangers pediatric health, CPF inhibits the activity of acetylcholinesterase, induces neuroimmune inflammatory response (Helali et al., 2016), and disrupts the nervous system function.

The relationship between CPF concentration and microglia cells in

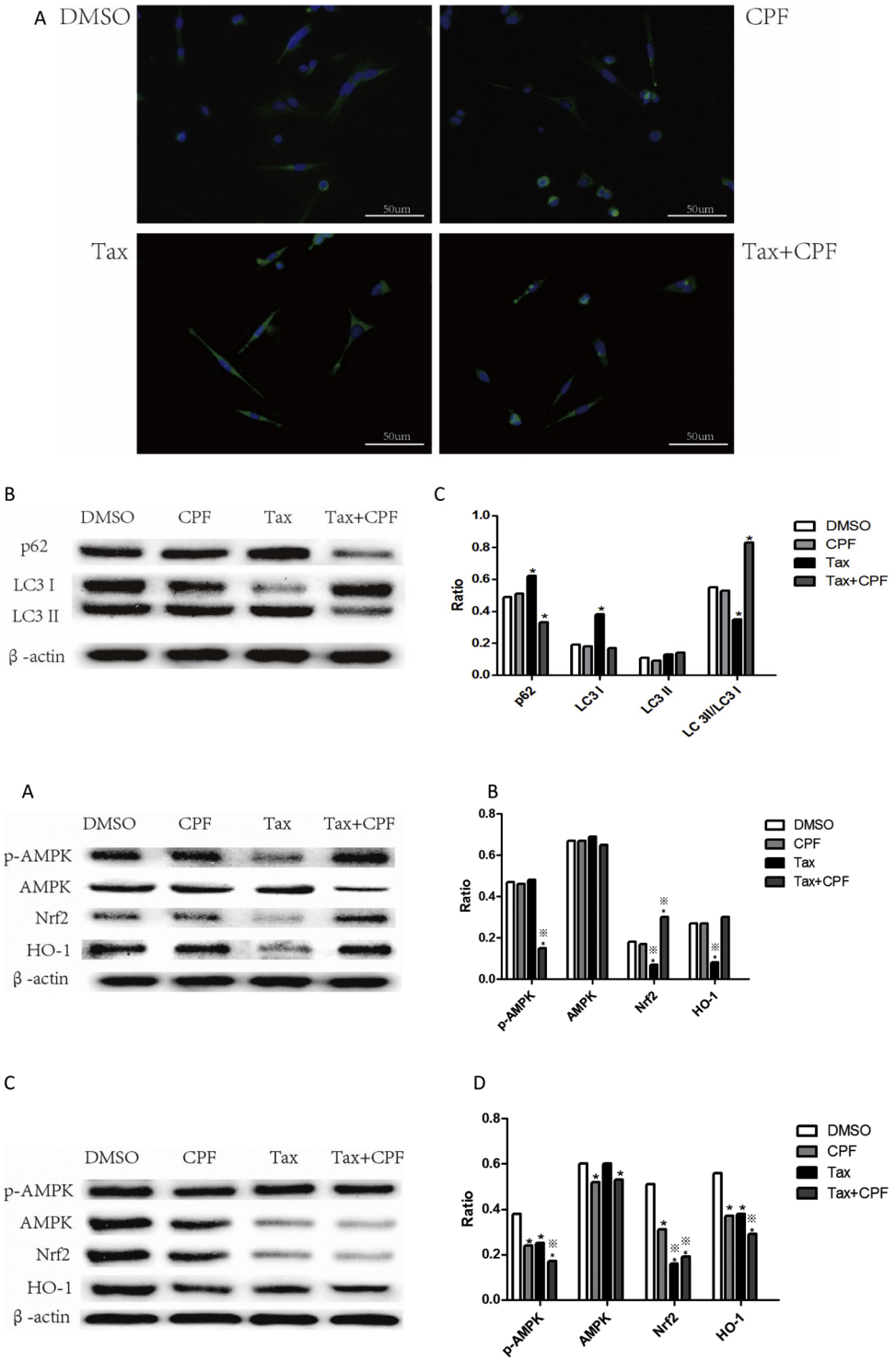

Fig. 5. Effect of Tax on autophagocytosis of BV2. Immunofluorescence staining was used to detect level of LC3 II in cells and positive antibody showed green. Protein expressions of p62 and LC3 II were determined by western blot method. **A**: IF detection of LC3 II expression in BV2 cells. LC3 II mainly expressed in cytoplasm. Compared with DMSO group, the expression of LC3 II in CPF group was not significantly increased in the cytoplasm, and the expression of LC3 II in both Tax and Tax + CPF group's cells increased in the cytoplasm. **B&C**: Tax effect of CPF on the expression of p62, LC3 protein in BV2 cells. Compared with the DMSO group, there was no significant difference in CPF group. The levels of p62 and LC3 II in Tax group were increased. The levels of p62 decreased in Tax + CPF group, while the expression level of LC3 II was increased ($P < 0.05$).* $P < 0.05$. (For interpretation of the references to colour in this figure legend, the reader is referred to the web version of this article).

Fig. 6. Effect of Tax on AMPK level and Nrf2/HO-1 pathway. Western blot method was used to determine the p-AMPK, AMPK, Nrf2, HO-1 protein expression of BV2 cells in each group with CPF induction, as well as the expression level of these proteins after blocking AMPK pathway by Compound C. **A&B.**: Tax effects of CPF on the expression of p-AMPK, AMPK, Nrf2, HO-1 protein in BV2 cells. The expression of AMPK, p-AMPK, Nrf2, HO-1 in CPF group were no significant change comparing with the DMSO group. The expression of AMPK and p-AMPK protein were increased in Tax group, while the expression of Nrf2 and HO-1protein were reduced. In Tax + CPF group, AMPK and p-AMPK protein expression were reduced, while the Nrf2 protein was higher expression, HO-1 protein was no significant increase in expression. Compared with CPF group, AMPK and p-AMPK proteins' expression were without significant increase in the Tax group, while the proteins expression of Nrf2 and HO-1were reduced. In the Tax + CPF group, there were reduction of p-AMPK protein expression, increase of Nrf2, unchanged of HO-1expression. **C&D**: Compound C on the expression of p-AMPK, AMPK, Nrf2, HO-1 protein in BV2 cells of each group. After the intervention of Compound C for 1 h, the expression of AMPK, p-AMPK, Nrf2 and HO-1 were reduced both in the CPF and Tax + CPF group, comparing with the DMSO group. The Tax group's protein expression of p-AMPK, Nrf2 and HO-1 were reduced ($P < 0.05$), but AMPK were without obviously change. Compared with the CPF group, AMPK and p-AMPK were relatively higher with lower of Nrf2 and HO-1 in the Tax group. In the Tax + CPF group, expression of AMPK slightly elevated but without statistically significant, while p-AMPK was relatively decreased, as well as Nrf2 and HO-1. *comparison with DMSO group $P < 0.05$, ※comparison with CPF group $P < 0.05$.

vitro, especially BV2, has not been reported. Otherwise, the harmful concentration of CPF in various cells are also different. Reyna's research used 50 μM or 100 μM CPF to treat JEG-3 cells (Reyna et al., 2017). In astrocyte-neuron co-cultures, 10–30 μM CPF was significative concentration (Wu et al., 2017). Shrestha mentioned that 6 mg/L and 12 mg/L CPF belongs to sub-toxic exposure concentration (Shrestha et al., 2018). Recently a member of our group has reported that viability of SH-SY5Y cells was inhibited by CPF in a dose-dependent manner (25, 50, 100, and 200 μM) (Zhao et al., 2019). Based on our pre-experiment, 200 μM CPF can induce morphology of BV2 cells changing distinctly without most cells dead. So we chose this concentration for our research.

Tax plays a role in the anti-oxidant, anti-inflammatory, and anti-allergic reactions by inhibiting and scavenging the free radicals (Ma

et al., 2012). Intriguingly (Wang et al., 2006), Tax was found to improve the cerebral ischemia reperfusion injury, and the mechanism might be attributed to the antioxidant effect mediated via the regulated cerebral ischemia-reperfusion injury of the NF-κB activity.

This study showed the toxic effect of CPF on BV2 cells: round morphology, cell synaptic atrophy, adhesion degeneration inducing cell aggregation gloating, and reduced cell survival rate. However, after Tax treatment, the activity and morphology of BV2 cells were improved. Thus, Tax exhibits a protective effect on the cells from CPF-induced damage. When we used Tax to treat BV2 for different time, the result shows that the cell activity was decline after 12 h and 24 h, comparing with blank group. Therefore we chose 6 h as time point for research to avoid Tax's effect of cell activity.

CPF and its metabolites damage tissues and cells through various biochemical pathways. Saulsbury reported that CPF can increase the production of NO in oligodendrocytes leading to oxidative stress (Saulsbury et al., 2009). Our pre-study showed that CPF induces inflammatory response by HMGB1/TLR4/Nox2 signal pathway in microglial cells (Tian et al., 2015). Apoptosis induced by CPF depends on ROS signal transduction pathway, such as MAPK pathway, which including JNK, p38 and ERK1/2 (Lee et al., 2012). CPF also leads to apoptosis by mitochondrial fragmentation, depolarization and excessive ROS production (Dai et al., 2015). And in SH-SY5Y cells, CPF induces mitochondrial autophagy mediated by PINK1/ Parkin。

Oxidative stress is a major component of CPF injury. Previous studies have shown that ROS generation may be major cause of genotoxicity, cell cycle perturbations, and apoptosis due to co-exposure with low doses of CPF (Chauhan et al., 2016). In this study, compared with DMSO group, ROS in CPF group were significantly increased. It confirms that CPF induces oxidative stress in BV2 cells. When the level of ROS is more than the natural antioxidant capacity, the structural and functional molecules can attack, modify, and damage the tissue. ROS is produced in large quantities, which can consume the endogenous antioxidant enzyme in the body, causing the expression and activity changes of various enzymes. The activity of antioxidant enzymes is decreased, and the removal ability of ROS in the brain tissue is decreased, resulting in its excessive accumulation that eventually led to lipid, protein, DNA oxidation, energy metabolism disorder, and cell death (Liu et al., 2015b). Compared with CPF group, ROS significantly decreased in Tax + CPF group, and the difference was statistically significant. It proves that Tax significantly reduces the oxidative stress response from CPF injury.

In the current study, the levels of TNF-α and IFN-γ were detected by ELISA and were found to be significantly increased under CPF treatment, but declined after Tax treatment. Thus, Tax can significantly reduce the CPF-induced inflammatory response of BV2 cells. Different types of stimulation can activate the microglia, including classic pro-inflammatory stimulus (such as fat polysaccharide and IFN-γ), environmental toxins (such as pesticides, heavy metals, and air pollutants), pathological neural degeneration (such as α-synuclein and Aβ), and nerve damage, which in turn, trigger a series of host defense signals (Dutta et al., 2012; Levesque et al., 2010). In the inflammatory response of the central nervous system, microglial cells release a large number of inflammatory mediators, including cytokines such as tumor necrosis factor α (TNF-α) (Binukumar et al., 2011).

LC3 is closely related to mammalian autophagy and is classified as type I and type II. LC3 I is distributed in the cytoplasm. In the process of autophagy, the combined system of Atgl2-At95 and ubiquitin sample enzymes E1, E2, Ap97p, Ap93p, partially change LC3 I to LC3 II that tightly combines with autophagy and autophagy-lysosome membrane until the completion of autophagy. Since LC3 I and LC3 II are present throughout the process of autophagy, they are considered as the biological markers of autophagy. We can not only detect autophagy by LC3 I and LC3 II but also compare their relative expression to deduce the strength of the process (Kabeya et al., 2004; Mizushima, 2004; Tanida et al., 2005; Tanida, 2011). The p62 is one of the selective substrates of autophagy. Current studies showed that p62 is co-localized with LC3, and hence, immunoprecipitated with LC3. p62 interacts with LC3 through LIR (Noda et al., 2010). The LIR of p62 in human is involved in autophagy degradation of p62 and the ubiquitin protein (Johansen and Lamark, 2011). A similar study was reported for the mouse p62 protein. The structural domain that interacts with LC3 is known as the LC3 recognition sequence (LRS) and is localized between the 334 and 342 amino acid residues in the p62 protein; it effectively combines with LC3 (Ichimura et al., 2008). p62 combines with PB1 structural domain for oligomerization, which is beneficial for the targeted entry of the molecule to the autophagy formation site associated with endoplasmic reticulum; the interaction with LC3 is involved in the formation of autophagy (Nezis and Stenmark, 2012). In this study, the Tax + CPF group had lower level of p62 protein but higher level of LC3 I than cells in CPF group. The increasing rate of LC3 II/LC3 I indicated abundant autophagosomes. As a substrate, the decrease in the level of p62 protein showed enhanced autophagy. This result suggested a protective role of Tax by promoting autophagy in the cells.

AMPK is a serine/threonine kinase and a sensor of cellular stress caused by ATP depletion and/or calcium imbalance. It can regulate the mitochondrial function, oxidative stress response, and autophagy, which plays a central role in the homeostasis of cell metabolism. The AMPK expression was found in neurons, glial cells, and vascular endothelial cells in the central nervous system. It is widely distributed in the central nervous system, rendering it as an effective neuroprotective target (Bright et al., 2009; Manwani and McCullough, 2013; Osuka et al., 2009). Nrf2/ARE is a critical endogenous antioxidant stress pathway. In physiological conditions, Nrf2 and the cytoplasmic protein KEAPL were combined to inhibit the activity. When cells were under oxidative stress, Nrf2 with KEAPL was translocated into the nucleus, where it combines with the oxidation reaction components ARE. Then, the expression of antioxidants and anti-inflammatory factors is induced to effectuate the function of resisting oxidative stress and anti-inflammation. *HO-1* is the target gene regulated by Nrf2/ARE pathway. The increase in HO-1 expression can enhance its antioxidant capacity, reduce the generation and release of inflammatory mediators, and inhibit the inflammatory response. Several studies confirmed that the activation of Nrf2/HO-1 signaling pathway can regulate inflammation, oxidative stress, and autophagy, which in turn, protects the brain injury (Blasi et al., 1990; Corradin et al., 1993; Ma et al., 2012). Whether the molecular mechanism of the protective effect of Tax on the neurotoxicity of BV2 cells induced by CPF is effectuated through the Nrf2/HO-1 pathway has not yet been reported. The expression of Nrf2/HO-1 was increased in the Tax + CPF group as compared to the CPF group. It suggests that Tax reduces oxidative stress in BV2 cells by improving the expression of Nrf2. To confirm the relationship between AMPK-Nrf2 − HO-1 signal pathway and Tax protection, we chose compound C, an AMPK inhibitor, to inhibit the protein expression of this pathway. After the intervention of Compound C for 1 h, compared with the CPF group, in the Tax + CPF group, expression of AMPK slightly elevated but without statistically significant, while p-AMPK was relatively decreased, as well as Nrf2 and HO-1. It means that, after CPF induced the damage, Tax executed a protective effect on the BV2 cells by downregulating the pAMPK level and activating the Nrf2/HO-1 pathway.

5. Conclusion

Tax serves as an antioxidant, improves the cell vigor, reduces inflammation and oxidative stress, and promotes autophagy. It plays a protective role on CPF-induced toxicity on BV2 cells. In addition, this protective mechanism might be dependent on the downregulation of pAMPK levels and the activation of Nrf2/HO-1 signaling pathways.

Conflict of interests

The authors declare that there are no conflicts of interest in the

present work.

Funding

This research received specific grant from "New Xiangya Talent Project" of the Third Xiangya Hospital of the Central South University (JY201524) and "Xiangya Famous Medical" project ([2014] No. 68).

References

Binukumar, B.K., Bal, A., Gill, K.D., 2011. Chronic dichlorvos exposure: microglial activation, proinflammatory cytokines and damage to nigrostriatal dopaminergic system. Neuromol. Med. 13, 251–265.
Blasi, E., Barluzzi, R., Bocchini, V., Mazzolla, R., Bistoni, F., 1990. Immortalization of murine microglial cells by a v-raf/v-myc carrying retrovirus. J. Neuroimmunol. 27, 229–237.
Bright, N.J., Thornton, C., Carling, D., 2009. The regulation and function of mammalian AMPK-related kinases. Acta Physiol. (Oxf) 196, 15–26.
Chauhan, L.K., Varshney, M., Pandey, V., Sharma, P., Verma, V.K., Kumar, P., Goel, S.K., 2016. ROS-dependent genotoxicity, cell cycle perturbations and apoptosis in mouse bone marrow cells exposed to formulated mixture of cypermethrin and chlorpyrifos. Mutagenesis 31, 635–642.
Corradin, S.B., Mauel, J., Donini, S.D., Quattrocchi, E., Ricciardi-Castagnoli, P., 1993. Inducible nitric oxide synthase activity of cloned murine microglial cells. GLIA 7, 255–262.
Dai, H., Deng, Y., Zhang, J., Han, H., Zhao, M., Li, Y., Zhang, C., Tian, J., Bing, G., Zhao, L., 2015. PINK1/Parkin-mediated mitophagy alleviates chlorpyrifos-induced apoptosis in SH-SY5Y cells. Toxicology 334, 72–80.
Dutta, G., Barber, D.S., Zhang, P., Doperalski, N.J., Liu, B., 2012. Involvement of dopaminergic neuronal cystatin C in neuronal injury-induced microglial activation and neurotoxicity. J. Neurochem. 122, 752–763.
Gupta, S.C., Mishra, M., Sharma, A., Deepak, B.T., Kumar, R., Mishra, R.K., Chowdhuri, D.K., 2010. Chlorpyrifos induces apoptosis and DNA damage in Drosophila through generation of reactive oxygen species. Ecotoxicol. Environ. Saf. 73, 1415–1423.
Helali, I., Ferchichi, S., Maaouia, A., Aouni, M., Harizi, H., 2016. Modulation of macrophage functionality induced in vitro by chlorpyrifos and carbendazim pesticides. J. Immunotoxicol. 13, 745–750.
Ichimura, Y., Kumanomidou, T., Sou, Y.S., Mizushima, T., Ezaki, J., Ueno, T., Kominami, E., Yamane, T., Tanaka, K., Komatsu, M., 2008. Structural basis for sorting mechanism of p62 in selective autophagy. J. Biol. Chem. 283, 22847–22857.
Johansen, T., Lamark, T., 2011. Selective autophagy mediated by autophagic adapter proteins. Autophagy 7, 279–296.
Jurewicz, J., Polanska, K., Hanke, W., 2013. Chemical exposure early in life and the neurodevelopment of children–an overview of current epidemiological evidence. Ann. Agric. Environ. Med. 20, 465–486.
Kabeya, Y., Mizushima, N., Yamamoto, A., Oshitani-Okamoto, S., Ohsumi, Y., Yoshimori, T., 2004. LC3, GABARAP and GATE16 localize to autophagosomal membrane depending on form-II formation. J. Cell. Sci. 117, 2805–2812.
Kaushik, S., Bandyopadhyay, U., Sridhar, S., Kiffin, R., Martinez-Vicente, M., Kon, M., Orenstein, S.J., Wong, E., Cuervo, A.M., 2011. Chaperone-mediated autophagy at a glance. J. Cell. Sci. 124, 495–499.
Kaur, S., Singla, N., Dhawan, D.K., 2019. Neuro-protective potential of quercetin during chlorpyrifos induced neurotoxicity in rats. Drug Chem. Toxicol. 42, 220–230.
Lee, J.E., Park, J.H., Shin, I.C., Koh, H.C., 2012. Reactive oxygen species regulated mitochondria-mediated apoptosis in PC12 cells exposed to chlorpyrifos. Toxicol. Appl. Pharmacol. 263, 148–162.
Levesque, S., Wilson, B., Gregoria, V., Thorpe, L.B., Dallas, S., Polikov, V.S., Hong, J.S., Block, M.L., 2010. Reactive microgliosis: extracellular micro-calpain and microglia-mediated dopaminergic neurotoxicity. BRAIN 133, 808–821.
Liu, P., Zhao, H., Wang, R., Wang, P., Tao, Z., Gao, L., Yan, F., Liu, X., Yu, S., Ji, X., Luo, Y., 2015a. MicroRNA-424 protects against focal cerebral ischemia and reperfusion injury in mice by suppressing oxidative stress. STROKE 46, 513–519.
Liu, Y., Zhang, L., Liang, J., 2015b. Activation of the Nrf2 defense pathway contributes to neuroprotective effects of phloretin on oxidative stress injury after cerebral ischemia/reperfusion in rats. J. Neurol. Sci. 351, 88–92.
Manwani, B., McCullough, L.D., 2013. Function of the master energy regulator adenosine monophosphate-activated protein kinase in stroke. J. Neurosci. Res. 91, 1018–1029.
Marks, A.R., Harley, K., Bradman, A., Kogut, K., Barr, D.B., Johnson, C., Calderon, N., Eskenazi, B., 2010. Organophosphate pesticide exposure and attention in young Mexican-American children: the CHAMACOS study. Environ. Health Perspect. 118, 1768–1774.
Mijaljica, D., Prescott, M., Devenish, R.J., 2011. Microautophagy in mammalian cells: revisiting a 40-year-old conundrum. AUTOPHAGY 7, 673–682.
Mizushima, N., 2004. Methods for monitoring autophagy. Int. J. Biochem. Cell Biol. 36, 2491–2502.
Nezis, I.P., Stenmark, H., 2012. p62 at the interface of autophagy, oxidative stress signaling, and cancer. Antioxid. Redox Signal. 17, 786–793.
Noda, N.N., Ohsumi, Y., Inagaki, F., 2010. Atg8-family interacting motif crucial for selective autophagy. FEBS Lett. 584, 1379–1385.
Osuka, K., Watanabe, Y., Usuda, N., Atsuzawa, K., Yoshida, J., Takayasu, M., 2009. Modification of endothelial nitric oxide synthase through AMPK after experimental subarachnoid hemorrhage. J. Neurotrauma 26, 1157–1165.
Ozkul, A., Akyol, A., Yenisey, C., Arpaci, E., Kiylioglu, N., Tataroglu, C., 2007. Oxidative stress in acute ischemic stroke. J. Clin. Neurosci. 14, 1062–1066.
Parran, D.K., Magnin, G., Li, W., Jortner, B.S., Ehrich, M., 2005. Chlorpyrifos alters functional integrity and structure of an in vitro BBB model: co-cultures of bovine endothelial cells and neonatal rat astrocytes. Neurotoxicology 26, 77–88.
Rauh, V.A., Garcia, W.E., Whyatt, R.M., Horton, M.K., Barr, D.B., Louis, E.D., 2015. Prenatal exposure to the organophosphate pesticide chlorpyrifos and childhood tremor. Neurotoxicology 51, 80–86.
Rauh, V.A., Garfinkel, R., Perera, F.P., Andrews, H.F., Hoepner, L., Barr, D.B., Whitehead, R., Tang, D., Whyatt, R.W., 2006. Impact of prenatal chlorpyrifos exposure on neurodevelopment in the first 3 years of life among inner-city children. Pediatrics 118, e1845–e1859.
Reyna, L., Flores-Martin, J., Ridano, M.E., Panzetta-Dutari, G.M., Genti-Raimondi, S., 2017. Chlorpyrifos induces endoplasmic reticulum stress in JEG-3 cells. Toxicol. In Vitro 40, 88–93.
Roncati, L., Termopoli, V., Pusiol, T., 2016. Negative role of the environmental endocrine disruptors in the human neurodevelopment. Front. Neurol. 7, 143.
Sasikala, C., Jiwal, S., Rout, P., Ramya, M., 2012. Biodegradation of chlorpyrifos by bacterial consortium isolated from agriculture soil. World J. Microbiol. Biotechnol. 28, 1301–1308.
Saulsbury, M.D., Heyliger, S.O., Wang, K., Johnson, D.J., 2009. Chlorpyrifos induces oxidative stress in oligodendrocyte progenitor cells. Toxicology 259, 1–9.
Shrestha, S., Singh, V.K., Sarkar, S.K., Shanmugasundaram, B., Jeevaratnam, K., Koner, B.C., 2018. Effect of sub-toxic chlorpyrifos on redox sensitive kinases and insulin signaling in rat L6 myotubes. J. Diabetes Metab. Disord. 17, 325–332.
Tanida, I., 2011. Autophagosome formation and molecular mechanism of autophagy. Antioxid. Redox Signal. 14, 2201–2214.
Tanida, I., Minematsu-Ikeguchi, N., Ueno, T., Kominami, E., 2005. Lysosomal turnover, but not a cellular level, of endogenous LC3 is a marker for autophagy. Autophagy 1, 84–91.
Tian, J., Dai, H., Deng, Y., Zhang, J., Li, Y., Zhou, J., Zhao, M., Zhao, M., Zhang, C., Zhang, Y., Wang, P., Bing, G., Zhao, L., 2015. The effect of HMGB1 on sub-toxic chlorpyrifos exposure-induced neuroinflammation in amygdala of neonatal rats. Toxicology 338, 95–103.
Wang, Y.H., Wang, W.Y., Chang, C.C., Liou, K.T., Sung, Y.J., Liao, J.F., Chen, C.F., Chang, S., Hou, Y.C., Chou, Y.C., Shen, Y.C., 2006. Taxifolin ameliorates cerebral ischemia-reperfusion injury in rats through its anti-oxidative effect and modulation of NF-kappa B activation. J. Biomed. Sci. 13, 127–141.
Wu, X., Yang, X., Majumder, A., Swetenburg, R., Goodfellow, F.T., Bartlett, M.G., Stice, S.L., 2017. From the cover: AstrocytesAre protective against chlorpyrifos developmental neurotoxicity in human pluripotent stem cell-derived astrocyte-neuron co-cultures. Toxicol. Sci. 157, 410–420.
Zhang, J., Zhao, L.L., Hu, Z.P., Zhou, J., Deng, L., Gu, F., Dai, H.M., Huang, M., 2011. [Effects of low-dose chlorpyrifos exposure on dopaminergic neurons in the midbrain substantia nigra and neural behavioral development in neonatal rats]. Zhongguo Dang Dai Er Ke Za Zhi 13, 989–994.
Zhao, M.W., Yang, P., Zhao, L.L., 2019. Chlorpyrifos activates cell pyroptosis and increases susceptibility on oxidative stress-induced toxicity by miR-181/SIRT1/PGC-1alpha/Nrf2 signaling pathway in human neuroblastoma SH-SY5Y cells: implication for association between chlorpyrifos and Parkinson's disease. Environ. Toxicol.